RESEARCH ARTICLE

Key Points:

- We compare two leaf photosynthesis models, based on different biophysical assumptions, that are both used in Earth system and weather modeling
- The two models calculate a near-similar response of net photosynthesis to light and CO_2 despite having considerable differences in their structure and process representation. This finding is significant across a wide range of naturally occurring photosynthetic capacities in vegetation
- Through a flowchart, a comparison of photosynthetic response to light and CO_2 and a parameter conversion table, we aim to enable more communication and exchange of data between users of the two models within the Earth system and weather modeling communities

Supporting Information:

Supporting Information may be found in the online version of this article.

Correspondence to:

K. H. H. van Diepen,
kevin.vandiepen@wur.nl

Comparison of C3 Photosynthetic Responses to Light and CO₂ Predicted by the Leaf Photosynthesis Models of Farquhar et al. (1980) and Goudriaan et al. (1985)

K. H. H. van Diepen[1,2] 🄳, **J. Goudriaan[2]**, **J. Vilà-Guerau de Arellano[2,3]** 🄳, **and H. J. de Boer[4]**

[1]Department of Plant Sciences, Horticulture and Product Physiology Group, Wageningen University, Wageningen, The Netherlands, [2]Meteorology and Air Quality Group, Wageningen University Research, Wageningen, The Netherlands, [3]Atmospheric Chemistry Department, Max Planck Institute for Chemistry, Mainz, Germany, [4]Department of Environmental Sciences, Faculty of Geosciences, Utrecht University, Utrecht, The Netherlands

Abstract The leaf photosynthesis models developed by Farquhar et al. (1980, https://doi.org/10.1007/BF00386231) (FvCB) and Goudriaan et al. (1985, https://doi.org/10.1007/978-1-4899-3665-3_10) (G85) are both used in Earth system and weather models to quantify ecosystem carbon assimilation. Despite their common role, a systematic comparison between these two photosynthesis models is currently lacking in scientific literature. In this technical report we compared the two models in a systematic way. Hereto we performed a comparative analysis of the model structures as well as the modeled responses of photosynthesis to light and CO_2 at leaf level. To facilitate future model comparison, we also constructed a lookup table that presents FvCB model parameters fitted to CO_2-response curves from G85 in a wide natural range in photosynthetic capacity at standardized temperature. The structure of the FvCB model differs fundamentally from the G85 model as the FvCB model considers rate-limiting processes due to Rubisco capacity, electron transport and triose phosphate utilization in parallel, whereas the G85 model considers Rubisco activity and triose phosphate utilization limitation to act in series scaled with quantum use efficiency. The models also differ fundamentally in terms of the parametrization of dark respiration. Still, both models calculate near-similar responses of photosynthesis to changes in light and CO_2 across a wide range in photosynthetic capacity with only two free parameters each. Our work thereby highlights functional similarities between these model approaches despite fundamental differences in model structure. Hence, standardized parameter sets that yield similar photosynthesis responses to light and CO_2 may facilitate intercomparison of Earth system and weather models.

Plain Language Summary In Earth system and weather models the exchange of CO_2 between the vegetation and the atmosphere is primarily determined by photosynthesis at leaf level. Two commonly applied representations of leaf photosynthesis are based on the models of Farquhar et al. (1980, https://doi.org/10.1007/BF00386231) (FvCB) and Goudriaan et al. (1985, https://doi.org/10.1007/978-1-4899-3665-3_10) (G85). A systematic comparison between the two model approaches is currently lacking in scientific literature. The objective of our technical report is to provide such a comparison and thereby to contribute to an exchange of ideas, data and applications between users of the respective models. We found that the two models calculate a similar response of net photosynthesis to light and CO_2, despite having considerable differences in their model structure and representation of physiological processes. The main difference in model structure is that the limitations to photosynthesis in the FvCB model are applied in parallel, whereas in the G85 model they are in series. We also present a lookup table to express parameters from the G85 model in terms of their equivalent FvCB parameters. This technical report thereby contributes to the comparison of models used across the Earth system and weather modeling communities.

1. Introduction

Plants exchange CO_2 with the atmosphere through the processes of photosynthesis and respiration (Smith & Dukes, 2013), thereby affecting the partitioning of surface fluxes in the carbon balances of the land and the atmosphere (Lasslop et al., 2010; Mahecha et al., 2010). In land surface models (LSMs), the exchange of CO_2 between the vegetation and the atmosphere is primarily determined by how photosynthesis is represented at leaf level (Knauer et al., 2020). LSM simulations of CO_2 exchange have repeatedly shown to be sensitive to

the physiological processes at the leaf level (e.g., Lemordant et al., 2018). Therefore, any representation of leaf photosynthesis requires detailed consideration when embedded in large scale modeling (Busch & Sage, 2017).

The most widely used model for leaf photosynthesis is the one developed by Farquhar, von Caemmerer and Berry (FvCB) (Farquhar et al., 1980), which is found in many LSMs used for Earth system modeling and appeared in four LSMs that participated in the fifth Coupled Model Intercomparison Project (CMIP) (Rogers, 2014; Rogers et al., 2017). The FvCB model predicts leaf photosynthesis mechanistically as the minimum of two biochemical limitations related to the kinetic properties of the Ribulose 1,5-biphosphate carboxylase-oxygenase (Rubisco) enzyme and to the transport of electrons as driven by light (Farquhar & von Caemmerer, 1982). Sometimes a third biochemical limitation is included that relates to the export of photosynthetic end-products called triose phosphate utilization (TPU) (Lombardozzi et al., 2018). An overview on applications and the different variants of the model can be found in von Caemmerer (2013) and Yin et al. (2021).

An alternative to the FvCB model is the leaf photosynthesis model of Goudriaan et al. (1985) (G85 model). The G85 model is based on phenomenological relationships of leaf photosynthesis and, similar to the FvCB model, it includes representations of the biochemical limitations by Rubisco, electron transport and TPU. The G85 model is traditionally used in meteorological research as part of the photosynthesis (A)-stomatal conductance (g_s) model of Jacobs (1994). This $A - g_s$ model has its main applications in the LSMs of the European Centre of Medium-Range Weather Forecasts (ECWMF) (Boussetta et al., 2013), of the Earth system model operated by the Centre National de Recherches Météorologiques (CNRM-ESM1) (Calvet et al., 1998; Masson et al., 2013; Séférian et al., 2016) and of the Dutch Atmospheric Large-Eddy Simulation (Vilà-Guerau de Arellano et al., 2014). Recently, the meteorological model of the ECMWF was used to model Earth system processes and the meteorological model CNRM-ESM1 was included in the sixth CMIP (Arora et al., 2020; Boussetta et al., 2021; Park et al., 2021). Thereby the G85 photosynthesis model has entered the Earth system modeling community.

The objective of this technical report is to provide a conceptual and quantitative comparison between the two models of photosynthesis. Our aim is to assess similarities and differences between the photosynthesis models and facilitate communication and exchange of data between their users. In our comparison, we considered the model parametrizations for C3 photosynthesis. Although the G85 model can be used for predicting C4 photosynthesis with adjustments in model parameters only (e.g., Szczypta et al., 2014), we argue that comparison of C4 photosynthesis responses of beyond the scope of this technical report.

Our technical report consists of three components. First, we design a flowchart that conceptually displays the structure of the two models and the way represented processes are coupled. Subsequently, we describe the behavior of the two models by comparing the predicted response of net photosynthesis (A_n) to the intercellular CO_2 concentration of the leaf (C_i) at constant photosynthetic active radiation (PAR) and to PAR at constant C_i. We do this since CO_2 and PAR are among the key environmental variables that determine A_n. Although we acknowledge the relevance of temperature and oxygen in shaping the response of photosynthesis, we argue that these factors fall outside the scope of the current analysis and have been discussed in previous studies in greater detail (e.g., Bernacchi et al., 2009; Sharkey, 1988). Finally, to facilitate future intercomparison and the extension to new processes in the representations, we provide a lookup table to enable users to switch back and forth between key parameters of the two models.

2. Materials and Methods

2.1. Research Strategy to Harmonize the Intercomparison

In the subsections that follow we provided for both models the equations through which leaf net photosynthesis is predicted. We only provided the equations that were used in our model comparison. We included the TPU limitation in the FvCB model as this limitation is by default integrated within the G85 model. We chose to use the model equations based on C_i since the majority of LSMs, in which these leaf photosynthesis models are nested, predict A_n based on C_i as well. Since leaf temperature and oxygen (O_2) do not alter the way in which net photosynthesis is calculated, we analyzed all model responses at constant leaf temperature of 25°C and at constant atmospheric oxygen of 0.21 mol(O_2) mol^{-1}(air).

Throughout this section we will present the equations of the two models in their respective standard unit: mass for the G85 model and moles for the FvCB model. This approach retains the parameter values that are commonly used in their respective communities. In Section 3, however, we present the results using units of moles to facilitate intercomparison.

2.2. FvCB Model

Farquhar et al. (1980) assume that the net photosynthetic rate (A_n; see Table S1 in Supporting Information S1 for all FvCB model variables) can be calculated as:

$$A_n = V_c - 0.5V_o - R_d \tag{1}$$

where V_c and V_o are the carboxylation and oxygenation rates of Ribulose 1,5-biphosphate (RuBP) as catalyzed by Rubisco, respectively. R_d is the leaf respiration during the day other than photorespiration (von Caemmerer, 2013), often termed as "dark respiration" (Lambers et al., 2008). V_c is the photosynthetic rate that is gross to R_d and photorespiration (Wohlfahrt & Gu, 2015), with the latter equal to half the rate of oxygenation since 0.5 mol of CO_2 is released for every mole of oxygen that is oxygenated. Photorespiration is assumed to occur in the mitochondria and not available for carboxylation (von Caemmerer et al., 2009). The use of V_o in the model is often circumvented by simplifying Equation 1 to (von Caemmerer, 2013):

$$A_n = V_c(1 - 0.5\varnothing) - R_d \tag{2}$$

where $\varnothing$ is the ratio of V_o to V_c and defined as (Farquhar et al., 1980):

$$\varnothing = \frac{2\Gamma^*}{C_i} \tag{3}$$

Here, Γ^* is the CO_2 compensation point in absence of dark respiration (Laisk, 1977): it is the internal CO_2 concentration of the leaf at which photorespiration is equal to photosynthesis gross to dark respiration.

Equations 1–3 form the basis of the model. To complete the model, V_c needs to be parametrized. Rubisco saturates relatively fast for its substrate RuBP, which has led to the formulation that V_c is either saturated by RuBP or limited by the regeneration of RuBP (Farquhar, 1979; Farquhar et al., 1980; Farquhar & von Caemmerer, 1982). The former case is also called the Rubisco limited rate of V_c, as the active Rubisco concentration is limiting when RuBP is saturating. The latter case is also called the electron-transport limited rate, as the transport of electrons drives RuBP regeneration (von Caemmerer et al., 2009). TPU limits photosynthesis when the other two rates are high and thereby sets the maximum rate that net photosynthesis can reach in the model (see Lombardozzi et al., 2018).

V_c is calculated as the minimum of three potential rates that relate to the above limitations (von Caemmerer, 2000):

$$V_c = \min\left(W_c, W_j, W_p\right) \tag{4}$$

with W_c the Rubisco limited rate of carboxylation, W_j the electron transport limited rate of carboxylation and W_p the gross rate of photosynthesis when limited by TPU.

Since Rubisco is both a carboxylase and oxygenase (Bowes et al., 1971), O_2 inhibits RuBP carboxylation and W_c is calculated using the Michaelis-Menten model for competitive inhibition (Badger & Andrews, 1974; Bowes & Ogren, 1972):

$$W_c = \frac{V_{\text{cmax}} C_i}{C_i + K_c \left(1 + \dfrac{O}{K_o}\right)} \tag{5}$$

where V_{cmax} is the maximum rate of carboxylation representing the catalyzing capacity of active Rubisco. K_c and K_o are the Michaelis-Menten constants of Rubisco to carboxylation and oxygenation, respectively. O is the O_2 concentration in the intercellular airspace of the leaf.

W_j is calculated according to (Farquhar et al., 1980):

$$W_j = \frac{JC_i}{4\left(C_i + 2\Gamma^*\right)} \tag{6}$$

where J is the rate of electron transport. The number 4 represents the four electrons that are required to assimilate one molecule of CO_2 in the Calvin-Benson cycle (Lambers et al., 2008). As J is utilized by both carboxylation and oxygenation, their ratio ($\varnothing$) determines the number of electrons available for carboxylation (Farquhar, 1979). The formulation of $\varnothing$ is hidden in Equation 6. J depends on absorbed PAR through the empirical equation of Farquhar and Wong (1984):

$$J = \frac{I_2 + J_{max} - \sqrt{\left(I_2 + J_{max}\right)^2 - 4\theta I_2 J_{max}}}{2\theta} \tag{7}$$

where I_2 is the absorbed PAR by photosystem II, J_{max} is the maximum electron transport rate and θ is a curvature factor (Evans, 1989). Recently, there are efforts to include a mechanistic description of electron transport in the FvCB model (e.g., Johnson & Berry, 2021; see; Yin et al., 2021). Yet, these efforts have not been included in Earth system models.

I_2 is subsequently defined as (von Caemmerer, 2013):

$$I_2 = \frac{PAR(1 - f)abs}{2} \tag{8}$$

where f is a loss factor that accounts for the spectral quality of light (von Caemmerer, 2013). abs is the absorbance efficiency of the leaf and smaller than 1 as some wavelengths within the wavelength range of PAR are absorbed at a low efficiency (Evans, 1987). PAR is the intercepted PAR by the leaf. The number 2 accounts for dividing PAR equally among photosystem II and photosystem I, whereas only photosystem II drives electron transport (von Caemmerer et al., 2009).

W_p can be parametrized in various ways. A common parametrization is the one of Sharkey (1985):

$$W_p = \frac{3T_p}{1 - 0.5\varnothing} \tag{9}$$

where T_p is the export rate of triose phosphates from the chloroplast. The factor $(1 - 0.5\varnothing)$ serves to make the parametrization gross to photorespiration (von Caemmerer, 2013).

Using Equation 3 to substitute $\varnothing$ in Equation 2 and using Equations 5, 6 and 9 to substitute V_c in Equation 2 yields the potential rates of photosynthesis net of photorespiration:

$$A_c = \frac{V_{cmax}\left(C_i - \Gamma^*\right)}{C_i + K_c\left(1 + \dfrac{O}{K_o}\right)} \tag{10}$$

$$A_j = \frac{J\left(C_i - \Gamma^*\right)}{4\left(C_i + 2\Gamma^*\right)} \tag{11}$$

$$A_p = 3T_p \tag{12}$$

Subsequently, A_n can be calculated according to (von Caemmerer, 2013):

$$A_n = \min\left(A_c, A_j, A_p\right) - R_d \tag{13}$$

where R_d is commonly parametrized as follows:

$$R_d = 0.015V_{cmax} \tag{14}$$

2.3. G85 Model

The G85 modeling approach is based on the two essential conditions, namely either light or CO_2 as the limiting factor, that together led to a representation of how photosynthesis responds to light (Jacobs, 1994). Subsequently, Goudriaan et al. (1985) assume that the net photosynthetic rate (A_n; see Table S2 in Supporting Information S1 for all G85 model variables) can be calculated empirically as:

$$A_n = (A_m + R_d) \left(1 - e^{-\left(\frac{\epsilon PAR}{A_m + R_d} \right)} \right) - R_d \tag{15}$$

where A_m is the Rubisco limited net rate of carboxylation, R_d the dark respiration, ϵ the initial quantum use efficiency and PAR the absorbed PAR by the leaf.

ϵ is the initial slope of the light response curve and calculated according to (Goudriaan et al., 1985):

$$\epsilon = \epsilon_0 \frac{C_i - \Gamma^*}{C_i + 2\Gamma^*} \tag{16}$$

where ϵ_0 is the maximum initial quantum use efficiency. The value of ϵ_0 is based on the theoretical quantum requirement of the Calvin-Benson cycle: at least 8 photons in the PAR wavelength range are required to assimilate one molecule of CO_2 (von Caemmerer & Farquhar, 1981). Goudriaan et al. (1985) lowered the theoretical maximum value of ϵ_0 to account for PAR absorption by non-chlorophyll leaf tissue. The fraction in Equation 16 accounts for the energy cost and CO_2 release (i.e., photorespiration) by oxygenation.

Equations 15 and 16, combined with the parametrization of A_m in Goudriaan et al. (1985), predict an unlimited net photosynthesis at high CO_2 and PAR. For that reason, Jacobs (1994) used the TPU limitation as an upper boundary to A_m:

$$A_m = A_{\text{mmax}} \left(1 - e^{-\left(\frac{g_m \rho (C_i - \Gamma^*)}{A_{\text{mmax}}} \right)} \right) \tag{17}$$

where A_{mmax} is the TPU limited net rate of photosynthesis, g_m the mesophyll conductance and ρ the air density. Note that this use of g_m has historically been common, but deviates from the current definition and use of mesophyll conductance (Knauer et al., 2019, 2020; Tholen et al., 2012). g_m represents the initial slope of the Rubisco limited rate and of the CO_2-response curve as well when PAR is not limiting. A_{mmax} is based on the parametrization of Collatz et al. (1991), although in the G85 model A_{mmax} is directly assigned a value and net of all leaf respiration while in Collatz et al. (1991) the TPU limited rate has an explicit parametrization and is still gross to dark respiration. The air density in Equation 17 is needed to correct for the units of the other variables.

The dark respiration remained unparametrized in Goudriaan et al. (1985) and was given a parametrization by Jacobs (1994) following Van Heemst (1986):

$$R_d = \frac{A_m}{9} \tag{18}$$

2.4. Model Parameters

To analyze the behavior of the two models we compared their calculated response of A_n to C_i at several levels of PAR and their calculated response of A_n to PAR at several levels of C_i. The CO_2-response curves were compared at the PAR levels of 150, 800 and 1,800 μmol$m^{-2}s^{-1}$ and the light-response curves at the C_i levels of 125, 280 and 2,000 ppm. Thus, in total, we constructed six response curves with each model. The PAR levels are equal to approximately 22, 175 and 394 Wm^{-2} using a conversion factor of 4.57 μmol J^{-1} (McCree, 1972).

We selected the PAR level of 1,800 μmol$m^{-2}s^{-1}$ since it is a commonly used level to represent a saturating light intensity during leaf gas exchange measurements. We choose the PAR level of 150 μmol$m^{-2}s^{-1}$ to represent shade conditions and the PAR level of 800 μmol$m^{-2}s^{-1}$ as intermediate. Similarly, the C_i level of 2,000 ppm is chosen

Table 1
Parameter Values of the G85 Model, as in Jacobs (1994), and the FvCB Model Corresponding to a Reference Leaf Temperature of 25°C

Model	Symbol	Unit	Parameter	Value
G85	Γ^*_{298}	mg(CO_2) kg^{-1}(air)	CO_2 compensation point at 298 K	68.5
	$A_{mmax298}$	mg(CO_2) m^{-2} s^{-1}	TPU limited net rate at 298 K	2.2
	g_{m298}	mm s^{-1}	Mesophyll conductance at 298 K	7
	ϵ_0	mg(CO_2) J^{-1}	Maximum initial quantum use efficiency	0.017
FvCB	$V_{cmax298}$	µmol(CO_2) m^{-2} s^{-1}	Maximum carboxylation rate at 298 K	143
	K_{c298}	µmol(CO_2) mol^{-1}(air)	Michaelis Menten constant for carboxylation at 298 K	404.9
	K_{o298}	mmolCO_2 mol^{-1}(air)	Michaelis Menten constant for oxygenation at 298 K	287.4
	Γ^*_{298}	µmol(CO_2) mol^{-1}(air)	CO_2 compensation point at 298 K	45
	R_{d298}	µmol(CO_2) m^{-2} s^{-1}	Dark respiration at 298 K	2.3
	J_{max298}	µmol(electrons) m^{-2} s^{-1}	Maximum rate of electron transport at 298 K	234
	α	mol(CO_2) mol^{-1}(electrons)	Quantum-use efficiency	0.24
	θ	-	Curvature factor	0.85

Note. G85 model parameters g_{m298} and $A_{mmax298}$ follow the temperature inhibition response of Collatz et al. (1992), which lowers their calculated values at 25°C. The air density in the G85 model was set to 1.18 kg m^{-3}, which corresponds to the air density of dry air in a standard atmosphere of 25°C. The non-fitted FvCB model parameter values of K_c, K_o and Γ^* in *fitaci* of Duursma (2015) originate from Bernacchi et al. (2001). The non-fitted parameter values of α and θ are given by Duursma (2015), where α is termed as quantum-use efficiency (mol(electrons) mol^{-1}(photons)). α has different units compared to ϵ of the G85 model. The multiplication αPAR can be used to substitute I_2 in Equation 7. The value of Γ^*_{298} is equal in the two models, but is presented in different units.

since it is commonly used to represent a saturating CO_2 concentration during leaf gas exchange measurements. At the other extreme, the C_i level of 125 ppm represents the minimum atmospheric CO_2 concentration during the last glacial period (Petit et al., 1991; Siegenthaler et al., 2005), using a typical ratio of 0.7 to convert from atmospheric CO_2 concentration to C_i. The C_i level of 280 ppm is chosen to represent current atmospheric CO_2 concentration (400 ppm), using the same ratio of 0.7.

To construct the response curves of the G85 model we used the set of parameter values given by Jacobs (1994) (Table 1), which is a commonly used set in the literature (Ronda et al., 2001). Subsequently, we used the R package *fitaci* of Duursma (2015) to fit the FvCB model to the CO_2-response curve of the G85 model at the PAR level of 1,800 µmol m^{-2} s^{-1}. The fitted parameter values for V_{cmax} and J_{max} were then used to construct the six response curves of the FvCB model (Table 1). A value for R_d of the FvCB model was obtained using a different approach which we explain in the next sub-section.

2.5. Parameter Conversion

In addition to fitting the FvCB model to G85 model with default parameters, we extended the comparison of the two models to capture the natural range in photosynthesis response curves (Walker et al., 2014; Wullschleger, 1993). Hereto we first constructed 36 different CO_2-response curves with the G85 model which, when expressed in terms of the FvCB parameters V_{cmax} and J_{max}, encompass the parameters ranges presented by Walker et al. (2014). These CO_2-response curve combined six different values of g_{m298} with six different values of $A_{mmax298}$ ranging from 2.8 to 9.6 mm s^{-1} (110–390 mmol m^{-2} s^{-1}) and 0.88 to 3.08 mgCO_2 m^{-2} s^{-1} (20–70 µmol m^{-2} s^{-1}), respectively. All CO_2-response curves were generated with otherwise standard parameters (Table 1) and a PAR of 1,800 µmol m^{-2} s^{-1}. Corresponding FvCB parameters V_{cmax} and J_{max} were fitted using the R package *fitaci* of Duursma (2015).

Aligning dark respiration between the two models proved problematic as dark respiration in the G85 model is a function of C_i through A_m and thus not constant along the CO_2-response curves like in the FvCB model. Therefore we prescribed R_d as a fraction of V_{cmax} that can be derived as a G85 model parameter through (Delire et al., 2020; Jacobs, 1994):

$$g_m = \frac{V_{cmax}}{\Gamma^* + K_c \left(1 + \dfrac{O}{K_o}\right)}$$

(19)
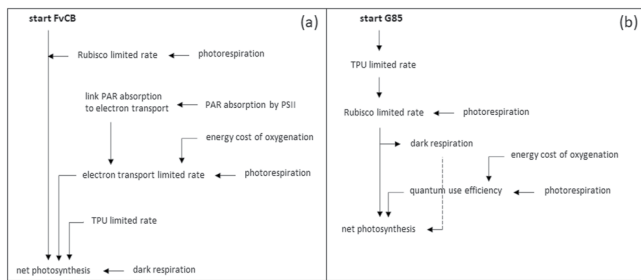
Figure 1. (a) Flowchart of the FvCB model equations and (b) G85 model equations. The arrows indicate the sequence in which the equations are solved. For explanation of the processes displayed in the chart: see Section 2.2 for the FvCB model and Section 2.3 for the G85 model.

Here, we used Γ^* of the G85 model and the Michaelis-Menten constants used for the FvCB model (Table 1). R_d was set equal to 0.015 V_{cmax} based on global-scale analyses (Atkin et al., 2015; Smith & Dukes, 2018; Wang et al., 2020).

2.6. Statistical Analyses

The goodness of fit between the CO_2-response curves of the two models was determined by the root mean square error (RMSE) and coefficient of determination (r^2). The RMSE was retrieved as a parameter from *fitaci*. The r^2 was obtained using MATLAB's linear regression model function *fitlm*, with r^2 based on Pearson's correlation coefficient.

3. Results

3.1. Model Structure

Although the G85 and FvCB models both aim to predict photosynthesis at the leaf level, we observed considerable differences in the model structure and the representation of processes. To visualize the model structure and how equations of separate processes are coupled we have developed a flowchart for each model (Figure 1). In case of the FvCB model, we choose to follow the model structure based on Equation 13 to predict net photosynthesis instead of Equations 2 and 4 since the former model structure is commonly present in LSMs (e.g., Bonan et al., 2011; Clark et al., 2011).

A fundamental property of the FvCB model is that photosynthesis is calculated from the combined limitations of Rubisco, electron transport and TPU (Figure 1a). Photorespiration is therefore considered in both Rubisco- and electron transport limited rates of photosynthesis. The TPU limitation is insensitive to photorespiration (McClain & Sharkey, 2019). The dark respiration subsequently is subtracted after the minimum of the three limitations is taken so that net photosynthesis is obtained. In the FvCB model, the Rubisco limited rate consists of an mechanistic representation of Rubisco enzyme kinetics that follows a rectangular hyperbola function. Its initial slope is given by Equation 19 (see also Equation 42 in Farquhar et al. [1980]). Both the initial slope and the saturation rate of the Rubisco limited rate scale linearly with V_{cmax}. The electron transport limitation consists of multiple processes coupled together. PAR represents the intercepted PAR by the leaf and reduces to absorbed PAR after accounting for the spectral quality of light and the absorbance efficiency of the leaf. Subsequently, the absorbed PAR is empirically related to electron transport rate following a non-rectangular hyperbola function. Lastly, the electron transport rate is reduced by a factor that accounts for the energy cost of oxygenation and for photorespiration. The conversion of absorbed PAR into a carboxylation rate is done in two steps: a factor 2 is used to convert absorbed PAR into electron transport rate and a factor 4 is used to convert electron transport rate into carboxylation rate. The initial slope of the electron transport limitation can be found by rewriting some of the formulations (Text S1 in Supporting Information S1). The saturation rate of the electron transport limited rate depends on J_{max}.

The limitations to photosynthesis in the G85 model are calculated in series and thereby coupled to each other (Figure 1b). The TPU limited net rate of photosynthesis serves as the maximum of the Rubisco limited net rate of carboxylation, which in turn determines maximum electron transport and saturates the light response. Therefore, A_{mmax} and A_m are potential net photosynthetic rates and the rate that results from the light response curve is the final net photosynthetic rate. Photorespiration is accounted for in two parts: once in the saturation part of the light response curve through the Rubisco limited rate and once in its initial slope through the quantum use efficiency. The dark respiration appears twice in the light response curve: once as an increment to A_m so that the factor ϵPAR saturates toward a photosynthetic rate gross to dark respiration and once as a subtraction to obtain net photosynthesis. In the G85 model the Rubisco limitation has an implicit representation of Rubisco enzyme kinetics through g_m and saturates toward A_{mmax} following a negative exponential function. The light-response curve follows a negative exponential function as well. The conversion of absorbed PAR into a carboxylation rate is done implicitly with the parameter ϵ_0. Its value is reduced by a factor that accounts for the energy cost of oxygenation and for photorespiration.

Few similarities exists between the two models in terms of structure and their representation of processes. An example is the representation of oxygenation, both its energy cost and its release of CO_2 (i.e., photorespiration). Additionally, some processes are represented differently but can be substituted into one another. For instance, the mesophyll conductance parameter of the G85 model can be explicitly calculated in terms of FvCB model parameters using Equation 19. For that reason, V_{cmax} of the FvCB model is represented through g_m in the G85 model. Similarly, ϵ_0 can be made explicit using FvCB model parameters (Text S1 in Supporting Information S1). Furthermore, both models use an empirical formulation to describe the transport of electrons driven by light.

There are some essential differences between the two models in terms of structure and process representation. The limitations to net photosynthesis in the FvCB model are applied in parallel, causing discontinuities at the transitions between the limitations (von Caemmerer et al., 2009). Since the limitations in the G85 model are in series, there is a smooth transition between them and not a discontinuity. The in-series applied limitations cause some processes to be absent in the G85 model. As the Rubisco limited rate saturates toward the TPU limitation, V_{cmax} is not represented in its saturation part. J_{max} is not at all represented in the G85 model as net photosynthesis saturates toward the Rubisco limitation. Finally, the two models parametrize dark respiration differently. In the G85 model dark respiration is a function of the Rubisco limited rate and thereby dependent on leaf temperature and C_i. Common parametrizations of dark respiration in the FvCB model cause dark respiration to be independent of C_i and merely a function of leaf temperature through V_{cmax}.

3.2. Model Behavior

By using FvCB model parameters fitted to a G85 CO_2-response curve, the FvCB and G85 models predict near-similar responses to combined changes in CO_2 and PAR (Figure 2). Although the FvCB model is fitted to the CO_2-response curve of the G85 model at a single level of saturating PAR, its fitted parameter values result in an accurate fit with varying C_i or PAR.

The calculated photosynthetic response of the two models to CO_2 follow a saturation type of curve that are similar in shape and magnitude (Figures 2a and 2b). The CO_2-response curves start at a negative value due to dark respiration and photorespiration. Although the dark respiration in the G85 model turns negative for C_i values below Γ^*, photorespiration pushes the net photosynthesis below zero. At a high PAR level (Figure 2a), net photosynthesis in the FvCB model is Rubisco limited for low values of C_i and subsequently becomes electron transport limited and TPU limited at higher values. Such transitions are not present along the CO_2-response curves of the G85 model: electron transport simply saturates toward the maximum rate set by the Rubisco limitation. At the combination of high C_i levels and high PAR levels, this maximum rate approaches the TPU limitation (A_{mmax}). At the intermediate PAR level (Figure 2b), the transition point in the FvCB model shifts to the left compared to the transition point at the high PAR level as the maximum rate of electron transport (J) drops. In the G85 model, the net photosynthesis at zero C_i increases a bit compared to net photosynthesis at zero C_i at the high PAR level. This occurs since the initial slope of the CO_2-response curve in the G85 model depends on PAR. If PAR is at an unsaturating level, net photosynthesis does not reach the maximum value set by the Rubisco limited rate and the initial slope will be less steep than it would be if PAR would be at a saturating level. At the low PAR level (Figure 2c), photosynthesis in the FvCB model is limited by electron transport over the whole range of C_i and the transition point between the Rubisco limitation and electron transport limitation has thus disappeared. Also, net photosynthesis at zero C_i has increased as the initial slope of the electron transport limited rate depends on PAR. The physical interpretation is that less electrons are available for both oxygenation and carboxylation, so that photorespiration is reduced for a given C_i.

Similar to the CO_2 responses, the calculated photosynthetic response of the two models to PAR follow a saturation type of curve and are similar in shape and magnitude (Figures 2d–2f). The light-response curves start at a negative value due to dark respiration. Whereas dark respiration in the FvCB model is constant at all three C_i levels, it is not in the G85 model: dark respiration increases with C_i and therefore net photosynthesis is most negative at the highest C_i level and least negative at the lowest C_i level. At the highest C_i level (Figure 2d), net photosynthesis in the FvCB model is electron transport limited for low to intermediate values of PAR and Rubisco limited for high values of PAR. At lower C_i levels (Figures 2e and 2f), the transition between these two limitation shifts to the left as the maximum Rubisco limited rate drops with C_i. The Rubisco limitation in the FvCB model imposes a sharp transition point onto net photosynthesis. Contrary to the CO_2-response curve, net photosynthesis does not
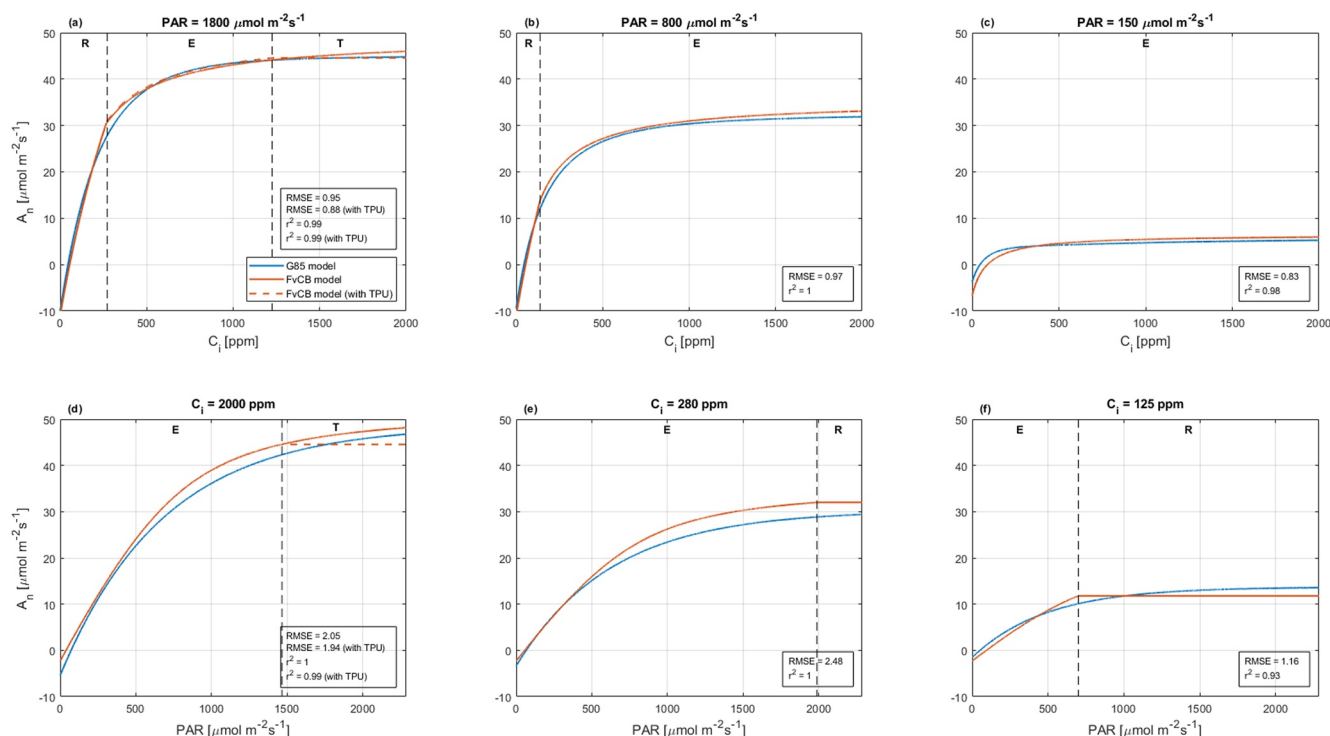
Figure 2. (a–c) CO_2-response curves and (d–f) light-response curves of the G85 model (blue), the FvCB model without TPU limitation (red) and the FvCB model including TPU limitation (red dashed). The CO_2-response curves range from a C_i level of 0–2,000 ppm and the light-response curve range from a PAR level of 0–2,285 μmol m^{-2} s^{-1} (or 500 W m^{-2}). The vertical dashed lines indicate the transition points between the limitations in the FvCB model. The letters R, E, and T indicate the Rubisco limitation, electron transport limitation and TPU limitation of the FvCB model, respectively. Statistical parameter values for the fits are given in the textboxes.

increase after the transition point as the Rubisco limitation is independent of PAR whereas the electron transport is not independent of C_i. As for the CO_2-response curves, this transition is not present along the light-response curve of the G85 model.

Despite using fitted FvCB model parameters, the two models cannot calculate an identical photosynthetic response to CO_2 or PAR. A crucial difference between the models is that the FvCB model has discontinuities at the transitions between the parallel limitations (for instance at 300 ppm in Figure 2a) and the G85 model does not have such discontinuities since its model structure considers limitations in series. The relative difference in net photosynthesis between the two models at the transition from Rubisco to electron-transport limited photosynthesis is around 10%. The difference in net photosynthesis at the transition between the electron transport limitation and TPU limitation of the FvCB model is negligible since this transition is located far into the saturation part of the CO_2-response curve. Furthermore, dark respiration in the G85 model is a function of C_i which causes an additional non-linearity that is not present in, and cannot be reproduced by, the CO_2-response curve of the FvCB model.

3.3. Parameter Conversion

The CO_2-response curves of the two models show a high goodness of fit over the whole range of combinations of the G85 model parameters g_m, R_d and A_{mmax} (Table 2). The coefficient of determination decreases slightly at high values of g_m combined with low values of A_{mmax}, but is high overall (≥0.99). The RMSE overall increases with g_m and is highest when g_m is combined with low values of A_{mmax}, similar to r^2. When comparing RMSE with A_{mmax}, it should be kept in mind that the unit of RMSE is a factor 22.73 (1,000/44) smaller than that of A_{mmax}.

There are a few relations between key parameters of the two models. V_{cmax} increases with g_m and remains approximately constant when g_m is combined with various values for A_{mmax}. Vice versa, J_{max} increases with A_{mmax}. When

Table 2
FvCB Model Parameters V_{cmax} *($\mu molCO_2\ m^{-2}\ s^{-1}$) and* J_{max} *(mol(electrons) $m^{-2}\ s^{-1}$) Fitted to 36 Combinations of the G85 Model Parameters* g_m *(mm s^{-1}),* A_{mmax} *($mgCO_2\ m^{-2}\ s^{-1}$) and* R_d *($mgCO_2\ m^{-2}\ s^{-1}$) at a PAR of 1,800 $\mu mol m^{-2} s^{-1}$*

g_m	R_d	A_{mmax}	V_{cmax}	J_{max}	J_{max}/V_{cmax}	r^2	RMSE
2.8	0.92	0.88	58.0	93.1	1.61	0.99	0.44
		1.32	58.8	134	2.29	1.00	0.62
		1.76	63.3	173	2.73	1.00	0.71
		2.2	68.2	208	3.05	1.00	0.63
		2.64	72.8	240	3.29	1.00	0.52
		3.08	76.9	268	3.49	1.00	0.56
4.2	1.38	0.88	92.4	98.2	1.06	0.98	0.85
		1.32	86.8	141	1.63	0.99	0.64
		1.76	86.1	181	2.11	0.99	0.83
		2.2	88.4	219	2.48	0.99	1.04
		2.64	91.4	252	2.76	0.99	1.17
		3.08	94.5	283	2.99	1.00	1.21
5.6	1.84	0.88	114	102	0.90	0.94	1.39
		1.32	124	147	1.18	0.99	0.95
		1.76	117	189	1.62	0.99	0.81
		2.2	113	227	2.01	0.99	1.00
		2.64	113	262	2.31	0.99	1.25
		3.08	115	294	2.56	0.99	1.46
7.0	2.30	0.88	144	105	0.73	0.91	1.83
		1.32	150	151	1.01	0.97	1.45
		1.76	151	194	1.29	0.99	1.02
		2.2	143	234	1.63	0.99	0.95
		2.64	140	270	1.93	0.99	1.14
		3.08	138	304	2.20	0.99	1.39
8.4	2.76	0.88	182	108	0.59	0.88	2.18
		1.32	168	155	0.92	0.95	1.92
		1.76	180	199	1.11	0.98	1.42
		2.2	178	240	1.35	0.99	1.07
		2.64	173	277	1.60	0.99	1.07
		3.08	165	312	1.89	0.99	1.25

A_{mmax} is combined with various values of g_m, J_{max} remains approximately constant although consistently increases by a small amount. Not surprisingly, the ratio of J_{max} to V_{cmax} increases with A_{mmax} for a given g_m.

4. Discussion

Although the leaf photosynthesis models of Farquhar et al. (1980) and Goudriaan et al. (1985) are currently used in Earth system and weather models, the two approaches have not been subject to any type of comparison yet. Despite fundamental differences in model structure, our results highlight that both models predict near-similar responses to light and CO_2 when common parameter sets are used. The validity of the mechanistic FvCB model to reproduce leaf-level responses in photosynthesis has been demonstrated extensively (e.g., Crous et al., 2013; Kattge & Knorr, 2007; Kumarathunge et al., 2019) and praised by many (Rogers, 2014; Rogers et al., 2017; Yin & Struik, 2009; Yin et al., 2021). The phenomenological G85 model has rarely been tested against leaf-level observations (Jacobs et al., 1996; Vilà-Guerau de Arellano et al., 2020). Yet, it appears in two well-known LSMs (Boussetta et al., 2013; Masson et al., 2013) that have recently been applied in a Earth system modeling context (Arora et al., 2020; Boussetta et al., 2021; Park et al., 2021).

The G85 models is a central component of the integrated $A - g_s$ model of Jacobs (1994) that comes with a comprehensive and versatile model infrastructure that is specifically designed for modeling canopy-level processes related to land-atmosphere exchange. These formulations consists of, among other things, an analytical method to upscale leaf gas exchange to the canopy (Ronda et al., 2001) and an elegant canopy radiative transfer scheme that includes the treatment of sunlit and shaded leaves (de Wit, 1965; Goudriaan, 1977, 1986; Pedruzo-Bagazgoitia et al., 2017). Additionally, $A - g_s$ is well-coupled to the atmosphere (Boussetta et al., 2013; Vilà-Guerau de Arellano et al., 2014) and, owing to its phenomenological character, its equations can be directly used to model both C3 and C4 vegetation (e.g., Szczypta et al., 2014). Altogether, it makes this $A - g_s$ model suitable to be integrated into LSMs for weather and Earth system modeling.

Although the two models calculate similar responses of net photosynthesis to CO_2 and PAR and can be fitted with excellent goodness of fit for a wide range of photosynthesis response curves using a limited set of parameters to cover the overall model parameter set, there are some considerable differences in model structure and process representation.

The FvCB model has discontinuities at the transitions between the limitations to net photosynthesis. This can result in computational problems when the model is used as sub-model embedded with other process representations (von Caemmerer et al., 2009). Observed responses of net photosynthesis to C_i show less prominent discontinuities (e.g., Wullschleger, 1993), likely as a result of spatial heterogeneity in leaf physiological properties and environmental conditions at the sub-leaf scale (Chen et al., 2008). Therefore the FvCB model may overestimate net photosynthesis around the transition points, which is especially relevant since recent optimality theory supports the hypothesis of the Rubisco- and electron transport limitations being coupled such that they colimit photosynthesis at C_i levels corresponding to atmospheric CO_2 concentrations (Wang et al., 2017).

Variants of the FvCB model that are commonly used in Earth system modeling avoid these discontinuities by smoothening the transitions between limitations. Collatz et al. (1991) do so using quadratic functions and Kull and Kruijt (1998) by using a mechanistic response of photosynthesis to light instead of an empirical one. Recently, Walker et al. (2021) compared the FvCB model with the Collatz et al. (1991) variant and found the

Table 2
Continued

g_m	R_d	A_{mmax}	V_{cmax}	J_{max}	J_{max}/V_{cmax}	r^2	RMSE
9.8	3.21	0.88	222	111	0.50	0.84	2.47
		1.32	194	159	0.82	0.93	2.33
		1.76	206	204	0.99	0.97	1.86
		2.2	208	245	1.18	0.99	1.37
		2.64	203	284	1.40	0.99	1.11
		3.08	196	320	1.63	0.99	1.14

Note. The vertical lines separate G85 model parameters (left), FvCB model parameters (middle) and statistical parameters of the fits (right). Each pair of g_m and R_d is combined with six different values of A_{mmax} yielding an equivalent amount of values for each FvCB model parameter and statistical parameter. The fits are done without including TPU in the FvCB model. In bold are the default G85 model parameter values. The RMSE is in units of $\mu molCO_2$ m^{-2} s^{-1}, similar to net photosynthesis. For quick data copying the values in Table 2 can be found in our repository: https://doi.org/10.5281/zenodo.6656163.

smoothening functions of the latter to significantly reduce net photosynthesis mainly around the transition points. On a global level, photosynthesis was reduced by 4%–10% because of that, demonstrating the risk of overestimating net photosynthesis by the FvCB model compared to observations. The G85 model has smooth transitions without having the need of additional smoothing functions as in Collatz et al. (1991).

The G85 model has dark respiration parametrized as the Rubisco limited rate divided by a factor 9. As a result, dark respiration is a function of C_i and turns negative when C_i drops below Γ^* and is about a threefold larger compared to observed rates of dark respiration at C_i levels representative of atmospheric CO_2 concentrations (Figure S1 in Supporting Information S1) (Bernacchi et al., 2001). Typically, dark respiration covaries with the photosynthetic capacity of a leaf (Lambers et al., 2008) and often is parametrized accordingly in the FvCB model and its variants. Therefore, it would be appropriate to decouple dark respiration and C_i in the G85 model and instead parametrize dark respiration as a fraction of A_{mmax}. In the past the model became numerically unstable around $C_i = \Gamma^*$ when dark respiration was parametrized as such. The instability occurred as the denominator and the numerator in Equation 15 did not turn zero at same value of C_i. We presume that the current parametrization of dark respiration was meant to circumvent model instability, although no confirmation of this can be found in Van Heemst (1986) or Jacobs (1994). Goudriaan et al. (1985) did not assign a parametrization to dark respiration, but they were not aware of potential model instability either. Within the $A - g_s$ model C_i increases under elevated atmospheric CO_2 concentration, causing dark respiration in the G85 model to increase as well. According to optimality theory and observations V_{cmax} decreases under elevated CO_2 (e.g., Harrison et al., 2021), providing support that dark respiration would decrease as well due to its tight link with V_{cmax}. Thereby, dark respiration in the G85 model behaves opposite to current knowledge.

Considering the enormous uncertainty that still exists in the magnitude of carbon-climate feedbacks in Earth system models (Spafford & MacDougall, 2021) we argue that the availability of fundamentally different model approaches capable of predicting near-similar responses in leaf-level photosynthesis can facilitate testing and model development via intercomparison. Differences between FvCB and G85-based photosynthesis schemes in future model intercomparison should be acknowledged while photosynthesis parameters between vegetation types can be aligned to minimize model variance due to inconsistent model input parameters. Eco-evolutionary optimality models of photosynthesis, stomatal conductance and gross primary production (GPP) provide potential opportunities to reduce the uncertainty in existing Earth system models. These optimality models have been developed around the FvCB model framework to predict photosynthesis parameters based on the least-cost hypothesis (Prentice et al., 2014; Smith et al., 2019; Stocker et al., 2020; Wang et al., 2017; Wright et al., 2003). The results are promising, but further work is needed to refine model formulations of stomatal conductance to environmental conductance, specifically soil moisture (Harrison et al., 2021). Application of optimality principles to the G85 and $A - g_s$ model formulations can potentially help in upscaling optimal stomatal responses from the leaf-level to the canopy level.

5. Conclusions

This technical report provides a comparison between the Farquhar et al. (1980) and Goudriaan et al. (1985) representations of leaf photosynthesis as part of Earth system and weather models. Our systematic comparison consisted of three components: a conceptual overview of the model structures, a quantitative comparison between the predicted responses of net photosynthesis to CO_2 and PAR, and a parameter conversion table. Despite having considerable differences in model structure and process representation, the two models predict a near-similar response of net photosynthesis to CO_2 and PAR. A main difference between the two models is that the Farquhar et al. (1980) model applies the limitations to net photosynthesis in parallel causing discontinuities at the transitions between these limitations. The model by Goudriaan et al. (1985) has no such discontinuities as the limitations are applied in series and scaled by quantum use efficiency. Second, the two models have a different

parametrization of dark respiration. The parametrization in the G85 model causes dark respiration to be a function of C_i and results in physically incorrect values at low levels of C_i and extremely high values at atmospheric CO_2 concentrations. Our work highlights the functional similarities between the model approaches despite their fundamental difference in model structure and thereby facilitate model testing and model intercomparison.

Conflict of Interest

The authors declare no conflicts of interest relevant to this study.

Data Availability Statement

The model scripts used to generate the results in this report are available at: https://doi.org/10.5281/zenodo.6656163.

References

Arora, V. K., Katavouta, A., Williams, R. G., Jones, C. D., Brovkin, V., Friedlingstein, P., et al. (2020). Carbon–concentration and carbon–climate feedbacks in CMIP6 models and their comparison to CMIP5 models. *Biogeosciences*, *17*(16), 4173–4222. https://doi.org/10.5194/bg-17-4173-2020

Atkin, O. K., Bloomfield, K. J., Reich, P. B., Tjoelker, M. G., Asner, G. P., Bonal, D., et al. (2015). Global variability in leaf respiration in relation to climate, plant functional types and leaf traits. *New Phytologist*, *206*(2), 614–636. https://doi.org/10.1111/nph.13253

Badger, M., & Andrews, T. (1974). Effects of CO_2, O_2 and temperature on a high-affinity form of ribulose diphosphate carboxylase-oxygenase from spinach. *Biochemical and Biophysical Research Communications*, *60*(1), 204–210. https://doi.org/10.1016/0006-291X(74)90192-2

Bernacchi, C., Singsaas, E., Pimentel, C., Portis, A., Jr., & Long, S. (2001). Improved temperature response functions for models of Rubisco-limited photosynthesis. *Plant, Cell and Environment*, *24*(2), 253–259. https://doi.org/10.1111/j.1365-3040.2001.00668.x

Bernacchi, C. J., Rosenthal, D. M., Pimentel, C., Long, S. P., & Farquhar, G. D. (2009). Modeling the temperature dependence of C3 photosynthesis. In *Photosynthesis in silico* (pp. 231–246). Springer.

Bonan, G. B., Lawrence, P. J., Oleson, K. W., Levis, S., Jung, M., Reichstein, M., et al. (2011). Improving canopy processes in the Community Land Model version 4 (CLM4) using global flux fields empirically inferred from FLUXNET data. *Journal of Geophysical Research*, *116*(G2), G02014. https://doi.org/10.1029/2010JG001593

Boussetta, S., Balsamo, G., Arduini, G., Dutra, E., McNorton, J., Choulga, M., et al. (2021). ECLand: The ECMWF Land Surface Modelling System. *Atmosphere*, *12*(6), 723. https://doi.org/10.3390/atmos12060723

Boussetta, S., Balsamo, G., Beljaars, A., Panareda, A.-A., Calvet, J.-C., Jacobs, C., et al. (2013). Natural land carbon dioxide exchanges in the ECMWF integrated forecasting system: Implementation and offline validation. *Journal of Geophysical Research: Atmospheres*, *118*(12), 5923–5946. https://doi.org/10.1002/jgrd.50488

Bowes, G., Ogren, W., & Hageman, R. (1971). Phosphoglycolate production catalyzed by ribulose diphosphate carboxylase. *Biochemical and Biophysical Research Communications*, *45*(3), 716–722. https://doi.org/10.1016/0006-291X(71)90475-X

Bowes, G., & Ogren, W. L. (1972). Oxygen inhibition and other properties of soybean ribulose 1, 5-diphosphate carboxylase. *Journal of Biological Chemistry*, *247*(7), 2171–2176. https://doi.org/10.1016/S0021-9258(19)45507-5

Busch, F. A., & Sage, R. F. (2017). The sensitivity of photosynthesis to O_2 and CO_2 concentration identifies strong Rubisco control above the thermal optimum. *New Phytologist*, *213*(3), 1036–1051. https://doi.org/10.1111/nph.14258

Calvet, J.-C., Noilhan, J., Roujean, J.-L., Bessemoulin, P., Cabelguenne, M., Olioso, A., & Wigneron, J.-P. (1998). An interactive vegetation SVAT model tested against data from six contrasting sites. *Agricultural and Forest Meteorology*, *92*(2), 73–95. https://doi.org/10.1016/S0168-1923(98)00091-4

Chen, C. P., Zhu, X.-G., & Long, S. P. (2008). The effect of leaf-level spatial variability in photosynthetic capacity on biochemical parameter estimates using the Farquhar model: A theoretical analysis. *Plant Physiology*, *148*(2), 1139–1147. https://doi.org/10.1104/pp.108.124024

Clark, D., Mercado, L., Sitch, S., Jones, C., Gedney, N., Best, M., et al. (2011). The Joint UK Land Environment Simulator (JULES), model description–Part 2: Carbon fluxes and vegetation dynamics. *Geoscientific Model Development*, *4*(3), 701–722. https://doi.org/10.5194/gmd-4-701-2011

Collatz, G. J., Ball, J. T., Grivet, C., & Berry, J. A. (1991). Physiological and environmental regulation of stomatal conductance, photosynthesis and transpiration: A model that includes a laminar boundary layer. *Agricultural and Forest Meteorology*, *54*(2), 107–136. https://doi.org/10.1016/0168-1923(91)90002-8

Collatz, G. J., Ribas-Carbo, M., & Berry, J. (1992). Coupled photosynthesis-stomatal conductance model for leaves of C4 plants. *Functional Plant Biology*, *19*(5), 519–538. https://doi.org/10.1071/PP9920519

Crous, K. Y., Quentin, A. G., Lin, Y. S., Medlyn, B. E., Williams, D. G., Barton, C. V., & Ellsworth, D. S. (2013). Photosynthesis of temperate Eucalyptus globulus trees outside their native range has limited adjustment to elevated CO_2 and climate warming. *Global Change Biology*, *19*(12), 3790–3807. https://doi.org/10.1111/gcb.12314

Delire, C., Séférian, R., Decharme, B., Alkama, R., Calvet, J. C., Carrer, D., et al. (2020). The global land carbon cycle simulated with ISBA-CTRIP: Improvements over the last decade. *Journal of Advances in Modeling Earth Systems*, *12*(9), e2019MS001886. https://doi.org/10.1029/2019MS001886

de Wit, C. T. (1965). Photosynthesis of leaf canopies.

Duursma, R. A. (2015). Plantecophys-an R package for analysing and modelling leaf gas exchange data. *PLoS One*, *10*(11), e0143346. https://doi.org/10.1371/journal.pone.0143346

Evans, J. (1987). The dependence of quantum yield on wavelength and growth irradiance. *Functional Plant Biology*, *14*(1), 69–79. https://doi.org/10.1071/PP9870069

Evans, J. R. (1989). Photosynthesis and nitrogen relationships in leaves of C3 plants. *Oecologia*, *78*(1), 9–19. https://doi.org/10.1007/BF00377192

Farquhar, G. D. (1979). Models describing the kinetics of ribulose biphosphate carboxylase-oxygenase. *Archives of Biochemistry and Biophysics*, *193*(2), 456–468. https://doi.org/10.1016/0003-9861(79)90052-3

Farquhar, G. D., Caemmerer, S. V., & Berry, J. A. (1980). A biochemical-model of photosynthetic CO_2 assimilation in leaves of C-3 Species. *Planta*, *149*(1), 78–90. https://doi.org/10.1007/BF00386231

Farquhar, G. D., & von Caemmerer, S. (1982). Modelling of photosynthetic response to environmental conditions. In O. L. Lange, P. S. Nobel, C. B. Osmond, & H. Ziegler (Eds.), *Physiological plant ecology II: Water relations and carbon assimilation* (pp. 549–587). Springer Berlin Heidelberg.

Farquhar, G. D., & Wong, S. C. (1984). An empirical model of stomatal conductance. *Functional Plant Biology*, *11*(3), 191–210. https://doi.org/10.1071/PP9840191

Goudriaan, J. (1977). *Crop micrometeorology: A simulation study*. Pudoc. Retrieved from https://edepot.wur.nl/166537

Goudriaan, J. (1986). A simple and fast numerical method for the computation of daily totals of crop photosynthesis. *Agricultural and Forest Meteorology*, *38*(1–3), 249–254. https://doi.org/10.1016/0168-1923(86)90063-8

Goudriaan, J., van Laar, H. H., van Keulen, H., & Louwerse, W. (1985). Photosynthesis, CO_2 and plant production. In W. Day & R. K. Atkin (Eds.), *Wheat growth and modelling* (pp. 107–122). Springer US. https://doi.org/10.1007/978-1-4899-3665-3_10

Harrison, S. P., Cramer, W., Franklin, O., Prentice, I. C., Wang, H., Brännström, Å., et al. (2021). Eco-evolutionary optimality as a means to improve vegetation and land-surface models. *New Phytologist*, *231*(6), 2125–2141. https://doi.org/10.1111/nph.17558

Jacobs, C. M. J. (1994). *Direct impact of atmospheric CO_2 enrichment on regional transpiration*. Jacobs. Retrieved from https://edepot.wur.nl/206972

Jacobs, C. M. J., van den Hurk, B. M. M., & de Bruin, H. A. R. (1996). Stomatal behaviour and photosynthetic rate of unstressed grapevines in semi-arid conditions. *Agricultural and Forest Meteorology*, *80*(2), 111–134. https://doi.org/10.1016/0168-1923(95)02295-3

Johnson, J., & Berry, J. (2021). The role of Cytochrome b6f in the control of steady-state photosynthesis: A conceptual and quantitative model. *Photosynthesis Research*, *148*(3), 101–136. https://doi.org/10.1007/s11120-021-00840-4

Kattge, J., & Knorr, W. (2007). Temperature acclimation in a biochemical model of photosynthesis: A reanalysis of data from 36 species. *Plant, Cell and Environment*, *30*(9), 1176–1190. https://doi.org/10.1111/j.1365-3040.2007.01690.x

Knauer, J., Zaehle, S., De Kauwe, M. G., Bahar, N. H., Evans, J. R., Medlyn, B. E., et al. (2019). Effects of mesophyll conductance on vegetation responses to elevated CO_2 concentrations in a land surface model. *Global Change Biology*, *25*(5), 1820–1838. https://doi.org/10.1111/gcb.14604

Knauer, J., Zaehle, S., De Kauwe, M. G., Haverd, V., Reichstein, M., & Sun, Y. (2020). Mesophyll conductance in land surface models: Effects on photosynthesis and transpiration. *The Plant Journal*, *101*(4), 858–873. https://doi.org/10.1111/tpj.14587

Kull, O., & Kruijt, B. (1998). Leaf photosynthetic light response: A mechanistic model for scaling photosynthesis to leaves and canopies. *Functional Ecology*, *12*(5), 767–777. https://doi.org/10.1046/j.1365-2435.1998.00257.x

Kumarathunge, D. P., Medlyn, B. E., Drake, J. E., Rogers, A., & Tjoelker, M. G. (2019). No evidence for triose phosphate limitation of light-saturated leaf photosynthesis under current atmospheric CO_2 concentration. *Plant, Cell and Environment*, *42*(12), 3241–3252. https://doi.org/10.1111/pce.13639

Laisk, A. K. (1977). Kinetics of photosynthesis and photorespiration of C3 in plants.

Lambers, H., Chapin, F. S., III, & Pons, T. L. (2008). *Plant physiological ecology*. Springer Science & Business Media.

Lasslop, G., Reichstein, M., Papale, D., Richardson, A. D., Arneth, A., Barr, A., et al. (2010). Separation of net ecosystem exchange into assimilation and respiration using a light response curve approach: Critical issues and global evaluation. *Global Change Biology*, *16*(1), 187–208. https://doi.org/10.1111/j.1365-2486.2009.02041.x

Lemordant, L., Gentine, P., Swann, A. S., Cook, B. I., & Scheff, J. (2018). Critical impact of vegetation physiology on the continental hydrologic cycle in response to increasing CO_2. *Proceedings of the National Academy of Sciences*, *115*(16), 4093–4098. https://doi.org/10.1073/pnas.1720712115

Lombardozzi, D. L., Smith, N. G., Cheng, S. J., Dukes, J. S., Sharkey, T. D., Rogers, A., et al. (2018). Triose phosphate limitation in photosynthesis models reduces leaf photosynthesis and global terrestrial carbon storage. *Environmental Research Letters*, *13*(7), 074025. https://doi.org/10.1088/1748-9326/aacf68

Mahecha, M. D., Reichstein, M., Carvalhais, N., Lasslop, G., Lange, H., Seneviratne, S. I., et al. (2010). Global convergence in the temperature sensitivity of respiration at ecosystem level. *Science*, *329*(5993), 838–840. https://doi.org/10.1126/science.1189587

Masson, V., Le Moigne, P., Martin, E., Faroux, S., Alias, A., Alkama, R., et al. (2013). The SURFEXv7.2 land and ocean surface platform for coupled or offline simulation of earth surface variables and fluxes. *Geoscientific Model Development*, *6*(4), 929–960. https://doi.org/10.5194/gmd-6-929-2013

McClain, A. M., & Sharkey, T. D. (2019). Triose phosphate utilization and beyond: From photosynthesis to end product synthesis. *Journal of Experimental Botany*, *70*(6), 1755–1766. https://doi.org/10.1093/jxb/erz058

McCree, K. J. (1972). Test of current definitions of photosynthetically active radiation against leaf photosynthesis data. *Agricultural Meteorology*, *10*, 443–453. https://doi.org/10.1016/0002-1571(72)90045-3

Park, S.-W., Kug, J.-S., Jun, S.-Y., Jeong, S.-J., & Kim, J.-S. (2021). Role of cloud feedback in continental warming response to CO_2 physiological Forcing. *Journal of Climate*, *34*(22), 8813–8828. https://doi.org/10.1175/jcli-d-21-0025.1

Pedruzo-Bagazgoitia, X., Ouwersloot, H., Sikma, M., Van Heerwaarden, C., Jacobs, C., & Vilà-Guerau de Arellano, J. (2017). Direct and diffuse radiation in the shallow cumulus–vegetation system: Enhanced and decreased evapotranspiration regimes. *Journal of Hydrometeorology*, *18*(6), 1731–1748. https://doi.org/10.1175/jhm-d-16-0279.1

Petit, J., White, J., Young, N., Jouzel, J., & Korotkevich, Y. S. (1991). Deuterium excess in recent Antarctic snow. *Journal of Geophysical Research*, *96*(D3), 5113–5122. https://doi.org/10.1029/90JD02232

Prentice, I. C., Dong, N., Gleason, S. M., Maire, V., & Wright, I. J. (2014). Balancing the costs of carbon gain and water transport: Testing a new theoretical framework for plant functional ecology. *Ecology Letters*, *17*(1), 82–91. https://doi.org/10.1111/ele.12211

Rogers, A. (2014). The use and misuse of V c, max in Earth System Models. *Photosynthesis Research*, *119*(1), 15–29. https://doi.org/10.1007/s11120-013-9818-1

Rogers, A., Medlyn, B. E., Dukes, J. S., Bonan, G., Von Caemmerer, S., Dietze, M. C., et al. (2017). A roadmap for improving the representation of photosynthesis in Earth system models. *New Phytologist*, *213*(1), 22–42. https://doi.org/10.1111/nph.14283

Ronda, R., De Bruin, H., & Holtslag, A. (2001). Representation of the canopy conductance in modeling the surface energy budget for low vegetation. *Journal of Applied Meteorology*, *40*(8), 1431–1444. https://doi.org/10.1175/1520-0450(2001)040<1431:ROTCCI>2.0.CO;2

Séférian, R., Delire, C., Decharme, B., Voldoire, A., Salas y Melia, D., Chevallier, M., et al. (2016). Development and evaluation of CNRM Earth system model–CNRM-ESM1. *Geoscientific Model Development*, *9*(4), 1423–1453. https://doi.org/10.5194/gmd-9-1423-2016

Sharkey, T. D. (1985). Photosynthesis in intact leaves of C3 plants: Physics, physiology and rate limitations. *The Botanical Review*, *51*(1), 53–105. https://doi.org/10.1007/BF02861058

Sharkey, T. D. (1988). Estimating the rate of photorespiration in leaves. *Physiologia Plantarum*, *73*(1), 147–152. https://doi.org/10.1111/j.1399-3054.1988.tb09205.x

Siegenthaler, U., Stocker, T. F., Monnin, E., Lüthi, D., Schwander, J., Stauffer, B., et al. (2005). Stable carbon cycle–climate relationship during the late Pleistocene. *Science*, *310*(5752), 1313–1317. https://doi.org/10.1126/science.1120130

Smith, N. G., & Dukes, J. S. (2013). Plant respiration and photosynthesis in global-scale models: Incorporating acclimation to temperature and CO_2. *Global Change Biology*, *19*(1), 45–63. https://doi.org/10.1111/j.1365-2486.2012.02797.x

Smith, N. G., & Dukes, J. S. (2018). Drivers of leaf carbon exchange capacity across biomes at the continental scale. *Ecology*, *99*(7), 1610–1620. https://doi.org/10.1002/ecy.2370

Smith, N. G., Keenan, T. F., Colin Prentice, I., Wang, H., Wright, I. J., Niinemets, Ü., et al. (2019). Global photosynthetic capacity is optimized to the environment. *Ecology Letters*, *22*(3), 506–517. https://doi.org/10.1111/ele.13210

Spafford, L., & MacDougall, A. H. (2021). Validation of terrestrial biogeochemistry in CMIP6 Earth system models: A review. *Geoscientific Model Development*, *14*(9), 5863–5889. https://doi.org/10.5194/gmd-14-5863-2021

Stocker, B. D., Wang, H., Smith, N. G., Harrison, S. P., Keenan, T. F., Sandoval, D., et al. (2020). P-Model v1. 0: An optimality-based light use efficiency model for simulating ecosystem gross primary production. *Geoscientific Model Development*, *13*(3), 1545–1581. https://doi.org/10.5194/gmd-13-1545-2020

Szczypta, C., Calvet, J.-C., Maignan, F., Dorigo, W., Baret, F., & Ciais, P. (2014). Suitability of modelled and remotely sensed essential climate variables for monitoring Euro-Mediterranean droughts. *Geoscientific Model Development*, *7*(3), 931–946. https://doi.org/10.5194/gmd-7-931-2014

Tholen, D., Ethier, G., Genty, B., Pepin, S., & Zhu, X. G. (2012). Variable mesophyll conductance revisited: Theoretical background and experimental implications. *Plant, Cell and Environment*, *35*(12), 2087–2103. https://doi.org/10.1111/j.1365-3040.2012.02538.x

Van Heemst, H. (1986). Potential crop production. In H. Van Keulen, J. Wolf, & W. Pudoc (Eds.), *Modelling of agricultural production: Weather, soil and crops*, *Simulation Monographs*.

Vilà-Guerau de Arellano, J., Ney, P., Hartogensis, O., De Boer, H., Van Diepen, K., Emin, D., et al. (2020). CloudRoots: Integration of advanced instrumental techniques and process modelling of sub-hourly and sub-kilometre land–atmosphere interactions. *Biogeosciences*, *17*(17), 4375–4404. https://doi.org/10.5194/bg-17-4375-2020

Vilà-Guerau de Arellano, J., Ouwersloot, H. G., Baldocchi, D., & Jacobs, C. M. (2014). Shallow cumulus rooted in photosynthesis. *Geophysical Research Letters*, *41*(5), 1796–1802. https://doi.org/10.1002/2014GL059279

von Caemmerer, S. (2000). *Biochemical models of leaf photosynthesis*. CSIRO Publishing.

von Caemmerer, S. (2013). Steady-state models of photosynthesis. *Plant, Cell and Environment*, *36*(9), 1617–1630. https://doi.org/10.1111/pce.12098

von Caemmerer, S., Farquhar, G., & Berry, J. (2009). Biochemical model of C3 photosynthesis. In *Photosynthesis in silico* (pp. 209–230). Springer.

von Caemmerer, S., & Farquhar, G. D. (1981). Some relationships between the biochemistry of photosynthesis and the gas exchange of leaves. *Planta*, *153*(4), 376–387. https://doi.org/10.1007/BF00384257

Walker, A. P., Beckerman, A. P., Gu, L., Kattge, J., Cernusak, L. A., Domingues, T. F., et al. (2014). The relationship of leaf photosynthetic traits–V_{cmax} and J_{max}–to leaf nitrogen, leaf phosphorus, and specific leaf area: A meta-analysis and modeling study. *Ecology and Evolution*, *4*(16), 3218–3235. https://doi.org/10.1002/ece3.1173

Walker, A. P., Johnson, A. L., Rogers, A., Anderson, J., Bridges, R. A., Fisher, R. A., et al. (2021). Multi-hypothesis comparison of Farquhar and Collatz photosynthesis models reveals the unexpected influence of empirical assumptions at leaf and global scales. *Global Change Biology*, *27*(4), 804–822. https://doi.org/10.1111/gcb.15366

Wang, H., Atkin, O. K., Keenan, T. F., Smith, N. G., Wright, I. J., Bloomfield, K. J., et al. (2020). Acclimation of leaf respiration consistent with optimal photosynthetic capacity. *Global Change Biology*, *26*(4), 2573–2583. https://doi.org/10.1111/gcb.14980

Wang, H., Prentice, I. C., Keenan, T. F., Davis, T. W., Wright, I. J., Cornwell, W. K., et al. (2017). Towards a universal model for carbon dioxide uptake by plants. *Nature Plants*, *3*(9), 734–741. https://doi.org/10.1038/s41477-017-0006-8

Wohlfahrt, G., & Gu, L. (2015). The many meanings of gross photosynthesis and their implication for photosynthesis research from leaf to globe. *Plant, Cell and Environment*, *38*(12), 2500–2507. https://doi.org/10.1111/pce.12569

Wright, I. J., Reich, P. B., & Westoby, M. (2003). Least-cost input mixtures of water and nitrogen for photosynthesis. *The American Naturalist*, *161*(1), 98–111. https://doi.org/10.1086/344920

Wullschleger, S. D. (1993). Biochemical limitations to carbon assimilation in C3 plants—A retrospective analysis of the A/C_i curves from 109 species. *Journal of Experimental Botany*, *44*(5), 907–920. https://doi.org/10.1093/jxb/44.5.907

Yin, X., Busch, F. A., Struik, P. C., & Sharkey, T. D. (2021). Evolution of a biochemical model of steady-state photosynthesis. *Plant, Cell and Environment*, *44*(9), 2811–2837. https://doi.org/10.1111/pce.14070

Yin, X., & Struik, P. (2009). C3 and C4 photosynthesis models: An overview from the perspective of crop modelling. *NJAS - Wageningen Journal of Life Sciences*, *57*(1), 27–38. https://doi.org/10.1016/j.njas.2009.07.001